Structure and dynamics of interacting Brownian particles in one-dimensional periodic substrates

2007 J. Phys.: Condens. Matter 19 226215

(http://iopscience.iop.org/0953-8984/19/22/226215)

IOP PUBLISHING JOURNAL OF PHYSICS: CONDENSED MATTER

J. Phys.: Condens. Matter **19** (2007) 226215 (13pp) doi:10.1088/0953-8984/19/22/226215

Structure and dynamics of interacting Brownian particles in one-dimensional periodic substrates

Salvador Herrera-Velarde and Ramón Castañeda-Priego

Instituto de Física, Universidad de Guanajuato, Loma del Bosque 103, Colonia Lomas del Campestre, 37150 León, Guanajuato, Mexico

E-mail: ramoncp@fisica.ugto.mx

Received 26 December 2006, in final form 20 April 2007
Published 14 May 2007
Online at stacks.iop.org/JPhysCM/19/226215

Abstract

We study both the structural and dynamic properties of charged colloids in one-dimensional periodic substrates. The dependence of the static structure and diffusion properties on the density and substrate parameters is investigated by means of Brownian dynamics simulations. We find that the competition between both particle–particle and particle–substrate interactions leads to a rich variety of adsorbate phases or particle distributions. We also demonstrate that the mean-square displacement, $W(t)$, at long times shows the typical non-Fickian behaviour, $W(t) \propto t^{1/2}$, even for periodic substrates. Moreover, we show that the depinning of the particles can be directly quantified through a loss of correlations in the structure or an enhancement of the particle mobility factor.

(Some figures in this article are in colour only in the electronic version)

1. Introduction

The study and understanding of dynamical processes that occur in systems exhibiting anomalous diffusive behaviour possess relevance in several disciplines ranging from physics and chemistry to biology and medicine. Anomalous diffusion is the occurrence of a mean-square displacement of the form $W(t) \equiv \langle \delta x^2(t) \rangle \propto t^{\alpha}$, where $\alpha \neq 1$. Depending on the anomalous diffusion exponent α, the motion can be either sub-diffusive ($0 < \alpha < 1$) or super-diffusive ($\alpha > 1$). Recently, fractional anomalous diffusion in systems subjected to periodic potentials has been investigated on the basis of the fractional Fokker–Planck equation [1].

In particular, the study of transport properties in quasi-one dimensions has become crucial to the understanding of many systems, such as highway traffic flows [2], microfluidic devices [3], transportation of adsorbate molecules through zeolites [4], among others. Usually, the transport in one-dimensional channels is called single-file diffusion (SFD). This concept has its origin in biophysics and allows us to account for the transport of water and ions through molecular-sized channels in membranes [5].

SFD is the process concerning diffusion of particles in confined quasi-one dimensional geometries where the particles exhibit random-walk movements in channels so narrow that no mutual passage is possible. As mutual passage is excluded, there is a correlation between subsequent displacements, so that the motion of individual particles requires the collective motion of many other particles in the same direction. Due to this restriction, the sequence of particles remains unaffected over all time t. These peculiarities are reflected in their diffusive behaviour, which presents strong deviations from normal diffusion.

Rigorous theoretical results for SFD have been derived in detail for the simple case of hard rod systems [6–8], where it is predicted that the mean-square displacement (MSD) for times much longer that the direct interaction time τ (i.e. the time that a particle needs to move a significant fraction of the mean particle distance) is given by the relation [9]

$$\lim_{t \gg \tau} W(t) = 2F\sqrt{t}, \tag{1}$$

where F is the so-called SFD mobility factor. This non-Fickian behaviour is a striking feature of SFD, in contrast to the linear increase with time in (open) systems with allowed mutual passage. Recently, Kollmann [10] demonstrated that relation (1) remains valid for colloidal and atomic systems independently of the nature of the interaction potentials for homogeneous systems in the fluid state, provided that the correlation length between the particles is of finite range and that the particles interact identically.

The experimental evidence confirming relation (1) was unavailable for a long time due to the lack of ideal experimental systems. The first experimental observations of SFD were realized in zeolitic materials, however the evidence of this process provided by different authors remains contradictory (see e.g. [11] and references therein). Nevertheless, Wei *et al* recently investigated the particle dynamics in narrow channels [12] by using quasi-one-dimensional paramagnetic colloids.

After the work of Wei *et al*, several experiments using colloidal systems have been carried out [13, 14]. In contrast with previous experiments, Lutz *et al* [11, 15] created 1D circular channels by means of scanning optical tweezers in order to avoid the presence of lateral confinement walls. This technique allows us to reduce the hydrodynamic interactions to have a higher mobility. This experimental setup allows us to elucidate the typical diffusion of suspended interacting charged particles in a free single file, i.e. in the absence of a substrate. However, there is no experimental evidence on the way in which a modulated substrate affects both the dynamics and structure of interacting particles along the channel. On the other hand, from the simulation point of view, Taloni and Marchesoni [16] investigated the mobility of point-like particles on periodic substrates. They found that the presence of the substrate does not invalidate the diffusion law (1).

In the present paper, we investigate both the structure and dynamics of charged colloidal particles in one-dimensional periodic substrates by means of Brownian dynamics (BD) as well as Monte Carlo (MC) computer simulations. This interesting and intriguing subject, as we will see further below, allows us to understand the physical properties, such as the particle distribution and the efficiency of particle transport, of Brownian interacting particles confined in narrow corrugated channels.

After the present introduction, in section 2 we describe the details of our model system and the simulation techniques employed in this work. Although the diffusive nature of charged colloids in a free single file is currently understood, in section 3 we summarize their main structural and dynamic properties. In section 4 the Frenkel–Kontorova model [17, 18] is briefly discussed to establish a direct connection with the structure of Brownian particles in different corrugated potential landscapes. Also, the mean-square displacement and the mobility factor

are analysed in terms of the substrate parameters. Finally, the paper is closed with a section of conclusions.

2. Model system and simulation techniques

2.1. Interaction between colloidal particles

Colloidal particles are present in a large variety of biological, chemical and physical systems. In the last few years, they have also been used as versatile model systems which allow us to understand fundamental processes in atomic systems or to elucidate problems in the context of statistical physics. Because the relevant interactions between colloids are easily and independently tunable, and the colloid position is accessible by means of optical techniques like video microscopy, they are used explicitly as well-controlled model systems. On the other hand, it has already been demonstrated that colloids exposed to periodic laser fields can serve as model systems for atomic monolayers [19].

Here we consider charged colloids with diameter σ. Then, after the hard-core interaction ($r > \sigma$), two colloidal particles separated by the distance r interact via the repulsive part of the DLVO pair potential,

$$\beta u(r) = Z_{\text{eff}}^2 \lambda_{\text{B}} \left[\frac{\mathrm{e}^{\kappa\sigma/2}}{1+\kappa\sigma/2} \right]^2 \frac{\mathrm{e}^{-\kappa r}}{r}, \tag{2}$$

where $\beta \equiv \frac{1}{k_{\text{B}}T}$ is the inverse of the thermal energy with k_{B} the Boltzmann's constant and T the temperature, Z_{eff} is the effective charge, λ_{B} is the Bjerrum length and κ is the Debye screening parameter. The values of the parameters used in equation (2) are $\sigma = 2.8$ μm, $Z_{\text{eff}} = 5400$, $\lambda_{\text{B}} = 0.72$ and $\kappa^{-1} = 550$ nm. These parameters were taken from [19].

2.2. Simulation techniques

The structure of the suspension is discussed in terms of the pair distribution function $g(x)$ and the static structure factor $S(q_x)$, while the diffusive behaviour is obtained from the MSD, $W(t)$. The $g(x)$ is computed by averaging on equilibrium configurations through the relation [20],

$$g(x) = \frac{1}{N\rho} \left\langle \sum_{i=1}^{N-1} \sum_{j>1}^{N} \delta(x - x_{ij}) \right\rangle, \tag{3}$$

where the angular brackets $\langle \cdots \rangle$ denote a statistical (temporal or ensemble) average, $\rho = N/L$ is the particle number density and N is the number of particles. Instead of the Fourier transform of the $g(x)$, the static structure factor is simulated by using the relation [20]

$$S(q_x) = N^{-1} \left\langle \left(\sum_{i=1}^{N} \cos(q_{x_i} \cdot x_i) \right)^2 + \left(\sum_{i=1}^{N} \sin(q_{x_i} \cdot x_i) \right)^2 \right\rangle, \tag{4}$$

where q_x is the magnitude of the wavevector. The MSD can be computed by means of the expression,

$$W(t) = \langle \Delta x(t)^2 \rangle = N^{-1} \sum_{i=1}^{N} \langle (x_i(t) - x_i(0))^2 \rangle. \tag{5}$$

The structural and dynamic properties given by equations (3)–(5) are then simulated by using the so-called Brownian dynamics simulation method without hydrodynamic interactions, which is based on Ermak's algorithm [21, 22],

$$x_i(t + \Delta t) = x_i(t) + \beta D_0 F_i(t) \Delta t + x_i^r(t), \tag{6}$$

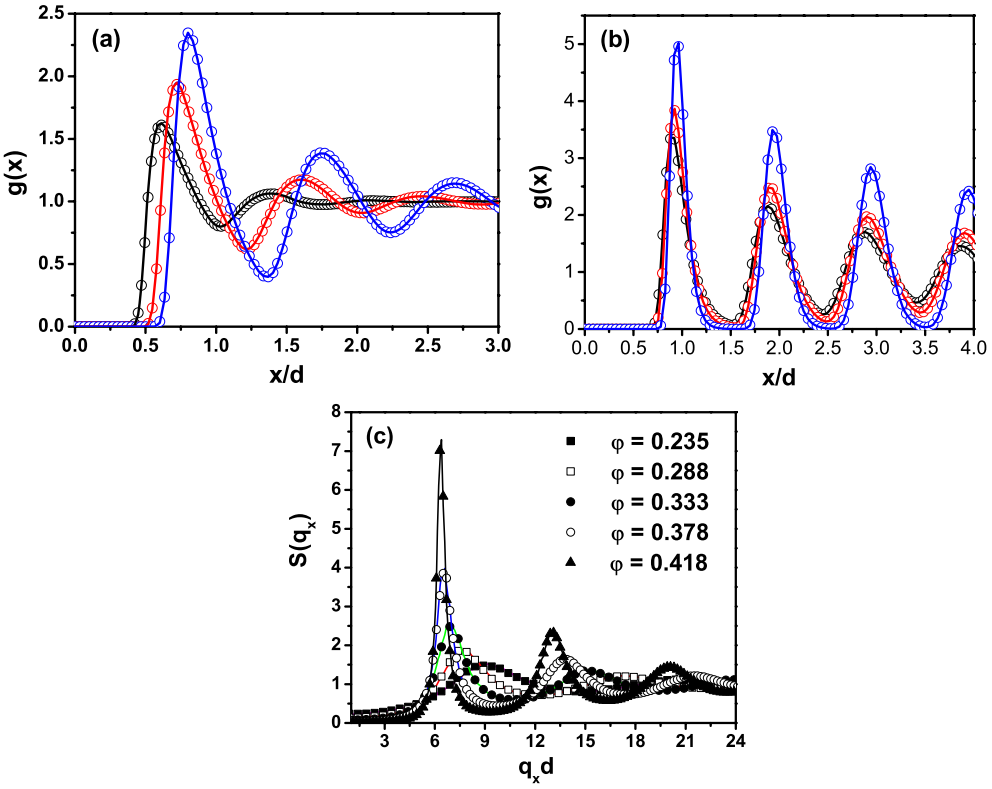

Figure 1. Pair distribution function, $g(x)$. (a) From left to right the packing fractions are $\varphi = 0.235$, 0.288 and 0.333. (b) From bottom to top the packing fractions are $\varphi = 0.4$, 0.418, and 0.458. (c) Static structure factor $S(q_x)$ (symbols) obtained from BD simulations. The structure is corroborated by means of MC simulations (solid lines).

where $x_i(t)$ denotes the position of the particle i at the time t, $F_i(t)$ is the total force acting on it due to its interaction with the other particles and the substrate, D_0 is the free-particle diffusion coefficient and $x_i^r(t)$ is a random displacement sampled from a Gaussian distribution with zero mean and width $\langle x_i^r(t)^2 \rangle = 2D_0\Delta t$.

In our simulations we move 900 particles according to Ermak's algorithm in a line of length L with periodic boundary conditions; movement in any other direction is not allowed. This model system tries to reproduce the same experimental conditions used in the experiments of Lutz *et al* [11, 15]. The time step used in our simulations is $\Delta t = 10^{-4}(\rho^2 D_0)^{-1}$. The structure is corroborated by standard Monte Carlo (MC) computer simulations [22]. A typical MC run consists of 1×10^6 steps to reach the thermalization and 5×10^6 steps to perform the statistics.

3. Charged colloids in a free single-file

Figures 1(a) and (b) show the pair distribution function, $g(x)$, of charged colloidal particles in a free single-file for different packing fractions, φ. One can observe that, for moderate densities (figure 1(a)), $g(x)$ takes the same properties of two- and three-dimensional interacting systems:

(i) as particles interact strongly repulsively at short distances, they do not feel the hard-core interaction, $g(r = \sigma) = 0$;

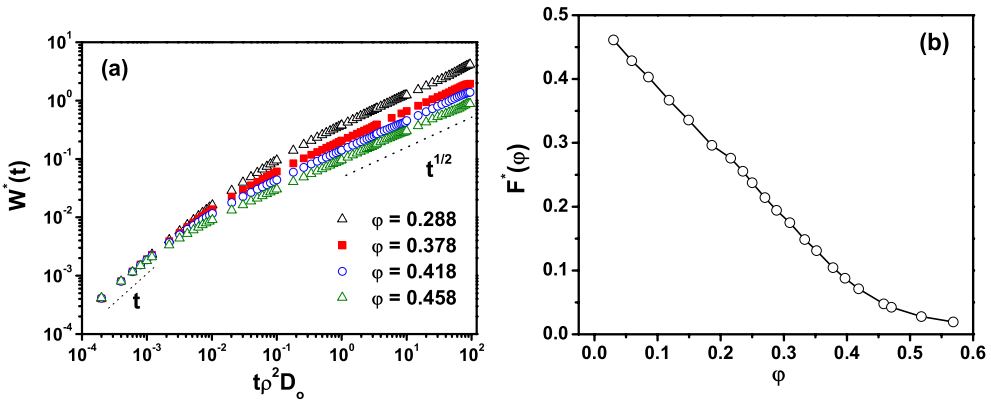

Figure 2. (a) Reduced mean-square displacement, $W^*(t)$, for different packing fractions obtained from BD simulations. (b) Reduced mobility factor F^* as a function of φ extracted from the fit to the simulation data according to relation (1). The solid line is just a guide for the eye.

(ii) it shows a typical fluid-like order, i.e. it decays to its corresponding ideal-gas value, $g(x) \approx 1$, according to the range of the interaction; and
(iii) particles are distributed uniformly in the whole space available.

However, at higher densities (figure 1(b)) the characteristic length scale of the system is determined by the mean interparticle distance, $d = \rho^{-1}$; the peaks are successively separated by the distance d. This fact is corroborated by the structure factor, $S(q_x)$, shown in figure 1(c), where the main peak is moving from right to left according to the bulk density until reaching the position $q_x d \approx 2\pi$. Our results are corroborated by Monte Carlo simulations (solid lines) which basically reproduce the same structural information.

The reduced mean-square displacement, $W^*(t) \equiv W(t)/d^2$, and the reduced single-file mobility factor, $F^* \equiv F\rho/D_0^{1/2}$, are shown in figures 2(a) and (b), respectively. The behaviour observed in both figures is in qualitative agreement with the experimental results of Lutz *et al* [11, 15]. At sufficiently short times, $t < 10^{-3}(\rho^2 D_0)^{-1}$, where the displacement of individual particles is governed by the interaction with the solvent, normal diffusion occurs and the MSD is found to be $W(t) \propto t$. By increasing the time, the presence of adjacent particles becomes more important until eventually a crossover occurs at times $t > 10^{-1}(\rho^2 D_0)^{-1}$, where $W(t)$ scales as $t^{1/2}$. The crossover time from normal diffusion to sub-diffusion occurs at earlier time as φ is increased. This is due to the fact that, on increasing the particle density, the direct particle–particle interaction becomes more important, including at shorter times.

The tendency shown by the MSD tells us that particles are accelerated linearly in time at short times, however at long times, after several particle collisions, particle acceleration is reduced, varying proportionally with $t^{1/2}$. This reduction in the particle acceleration is due to the energetic barrier imposed by the other neighbouring colloidal particles. On the other hand, the mobility decays with density in an exponential-like way (figure 2(b)). This monotonic behaviour has also been observed experimentally in zeolites at low temperatures [9] and recently in highly charged colloids [11, 15] and it is in qualitative agreement with an analytical expression derived for hard rods [9].

Due to the system being highly structured and the particle dynamics being practically suppressed at high densities, a possible liquid–solid-like transition is expected. However, further analysis in this direction is necessary to derive a static or dynamic criterion for

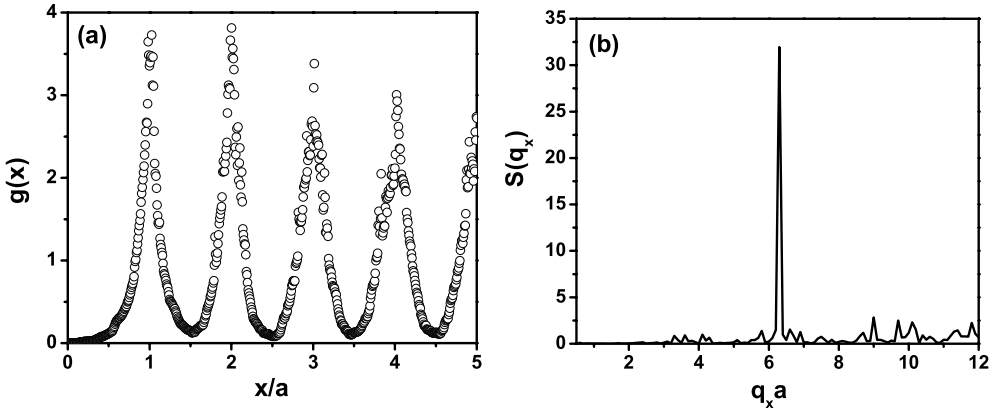

Figure 3. A typical (a) pair distribution function, $g(x)$, and (b) static structure factor, $S(q_x)$, in the Frenkel–Kontorova model for the case $K \neq 0$ and $V(x_n; b) = 0$.

determining the point of the liquid–solid transition in a system composed of interacting particles in a free single-file.

4. Brownian interacting particles on periodic substrates

4.1. Frenkel–Kontorova model

The simplest one-dimensional model for particles adsorbed on a periodic substrate was proposed by Frenkel and Kontorova. It provides a simple and realistic description of commensurate–incommensurate transitions when thermal fluctuations are unimportant, as they are near zero temperature [17, 18]. However, as we will see further below, thermal fluctuations play an important role in the system that we consider here, and hence cannot be completely neglected.

The adsorbed particles at positions x_n in the Frenkel–Kontorova (FK) model are treated as a harmonic chain with equilibrium lattice spacing a. The substrate is a one-dimensional periodic lattice with period b. The interaction between the nth adsorbed particle and the periodic substrate is described by a potential energy $V(x_n)$ characterized by the period b. The potential energy of the FK model is thus

$$U_{\mathrm{FK}} = \sum_n \left[\tfrac{1}{2}K\,(x_{n+1} - x_n - a) + V\,(x_n; b)\right]. \tag{7}$$

The first, or elastic, term in (7) favours a periodic lattice of adsorbed particles with $x_n = na$. This behaviour can be observed in the distribution function of figure 3(a) and its corresponding structure factor, figure 3(b), which shows a pronounced peak at the position $q_x a = 2\pi$. The second, or potential, term favours lock-in to the substrate, with each x_n an integral multiple of b. This case shows the same structural properties in terms of the structure functions, $g(x)$ and $S(q_x)$, as shown in figure 3 by replacing $a \to b$. If $V(x; b) = 0$, the adsorbate lattice spacing will be independent of b. The resulting structure is called a floating phase, in which the equilibrium lattice spacing a of the adsorbate lattice can be an arbitrary (including irrational) multiple of the substrate periodicity b. Thus, the floating phase is incommensurate for almost all values of the ratio a/b. In the opposite limit, where the potential is very large, one can expect each particle of the adsorbed lattice to sit in a minimum of the potential V. This leads to a commensurate structure, with the average spacing between adsorbate particle being a rational

multiple of b. For the case in which V is approximated by a cosine function, the rich FK phase diagram is described in detail in [18].

On the other hand, we consider a system where the adsorbed particles interact continuously through the potential given by equation (2). This means that each particle interacts not just with its nearest neighbor, as in the FK model. However, we expect to find structural properties similar to those already found in the FK model [18]. The energy potential of our system can then be written as

$$U = \sum_{i<j} u(x_{ij}) + \sum_{i} V_{\text{ext}}(x_i), \tag{8}$$

where the first term takes account of the pair interaction, while the second term describes the particle interaction with the periodic substrate,

$$V_{\text{ext}}(x; a_L) = V_0 \sin\left(\frac{2\pi x}{a_L}\right), \tag{9}$$

V_0 being the substrate strength, x the particle position, and a_L the substrate periodicity.

4.2. Structure

To characterize the structural properties fully, we determine both the pair correlation function and the static structure factor by varying the substrate parameters, V_0 and a_L, and the packing fraction, φ.

As already discussed in the last section, in the absence of the substrate ($V_0 = 0$) and at high densities ($\varphi \geqslant 0.4$) we found that the colloids form a highly ordered fluid with the mean particle distance $d = \rho^{-1}$ as the characteristic length scale (see figure 1(b)). From d we define the ratio $p \equiv d/a_L = \varphi^{-1}(\frac{\sigma}{a_L})$, which allows us to characterize the resulting type of commensurate, or incommensurate, structure. Initially, V_0 was chosen to be sufficiently small in order to allow particle fluctuations across the substrate barriers, i.e. to reach thermal equilibrium properly. Then V_0 was gradually increased until reaching the desired value.

Figure 4(a) shows the correlation function (symbols) for the case $a_L = \sigma$ with $\varphi \approx 0.407$, which corresponds to $p \approx 2.45$ for three different substrate strengths: $V_0 = 1.2$, 2.0 and 3.6 $k_{\text{B}}T$. For the sake of the discussion, we also plot the positions of the peaks (solid lines) corresponding to the case $V_0 = 0$ (multiples of $d \approx 2.45\sigma$). From the figure, one clearly observes that the substrate induces changes in the local structure of the suspension. In general, one can describe the following similar features:

(i) the peaks are slightly shifted with respect to the case without the substrate;
(ii) the substrate induces correlations among particles at separations smaller than d due to there being almost three substrate periods for each mean separation; and
(iii) both the shift in the peak positions around d and the particle correlations become stronger with the substrate strength.

As V_0 increases, the tendency of adsorbed particles to seek potential minima also increases. Nevertheless, the values of V_0 chosen in this work are not sufficiently large to favour a periodic lattice of adsorbed particles on each substrate minimum. Nonetheless, the competition between both contributions in equation (8) leads to a rich variety of adsorbate phases or particle distributions. For instance, one can notice that the nearest neighbour is closer to any central particle than in the case without a substrate, whereas the second neighbour becomes closer to the first one but is further from the third one. This interesting phenomenon can be visualized better in the static structure factor $S(q)$, which gives relevant information about the length scales of the system by looking at the position of its peaks. In figure 4(b) we show $S(q)$ for

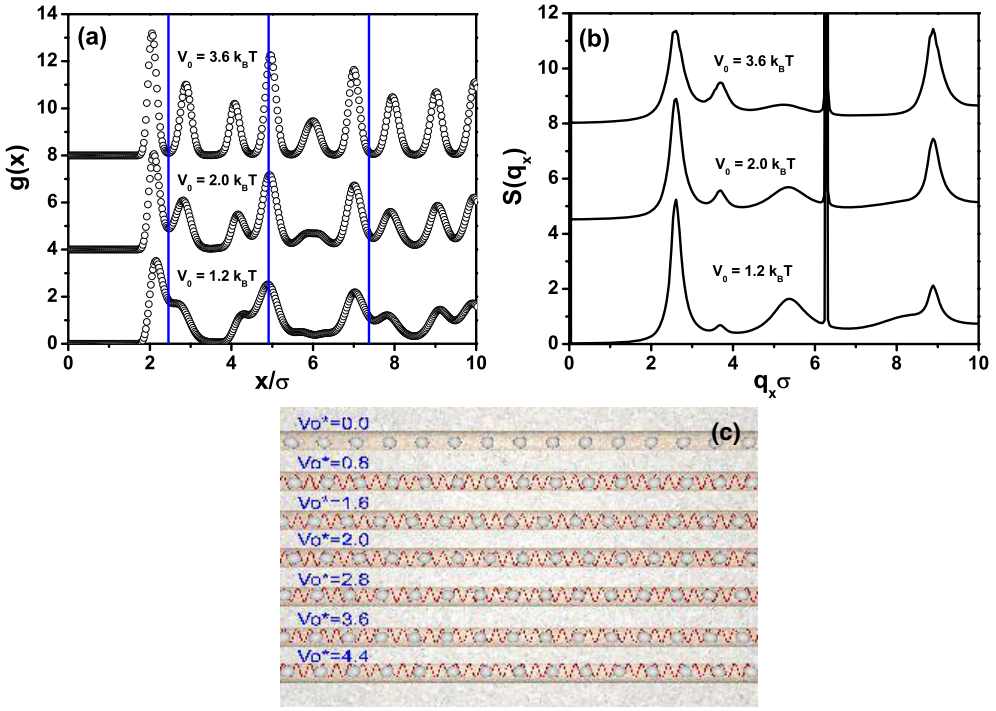

Figure 4. (a) Pair distribution functions for the case $a_L = \sigma$ with $\varphi \approx 0.407$ for three different substrate strengths: $V_0 = 1.2$, 2.0 and 3.6 k_BT. The perpendicular solid lines represent the position of each maximum for the case $V_0 = 0$. (b) Static structure factors. The curves are shifted for clarity. (c) Average configuration of the particles along the channels. From top to bottom, the substrate strengths are $V_0/k_BT = 0$, 0.8, 1.6, 2.0, 2.8, 3.6 and 4.4. The sinusoidal term of equation (9) is plotted (dashed lines) on each channel to understand the way in which the particles are positioned with respect to the substrate minima.

the systems of figure 4(a). One can distinguish three peculiar peaks at the following positions: (i) $q_x\sigma \approx 2.6$—this peak is related to the position of the first peak of the $g(x)$; (ii) $q_x\sigma = 2\pi$—such a peak is linked to the substrate periodicity; and (iii) $q_x\sigma \approx 8.9$—this peak progressively increases with V_0 and is directly involved with the separation between the first and second neighbour. Then the peaks at the positions $q_x\sigma \approx 2.6$ and $q_x\sigma \approx 8.9$ reveal that two adsorbed particles can be further and closer, respectively, than the distance between two consecutive substrate minima. These kinds of particle distribution have also been observed in the Frenkel–Kontorova model (see, e.g., [18]) and are called discommensurations because they break the commensurate registry of the adsorbate and substrate lattices. However, the height of the peak at $q_x\sigma = 2\pi$ indicates that there are regions on the substrate where the particles are located on the substrate minima. This happens at large distances, where the structural order is basically dominated by the substrate periodicity because the pair interaction is practically turned off at large separations. Figure 4(c) shows the snapshots of the average particle positions.

The case $a_L = 2\sigma$ ($p \approx 1.23$) shows similar structural properties to the case discussed previously (data not shown). As a_L changes, new types of incommensurate structures are observed. Also, new length scales are found.

So far, we have analysed systems in which the substrate periodicity is smaller than d or $p > 1$. In such cases the incommensurate phases show similar structural properties. We now look at the case $p < 1$. This case is illustrated in figure 5 for $a_L = 3\sigma$ or equivalently

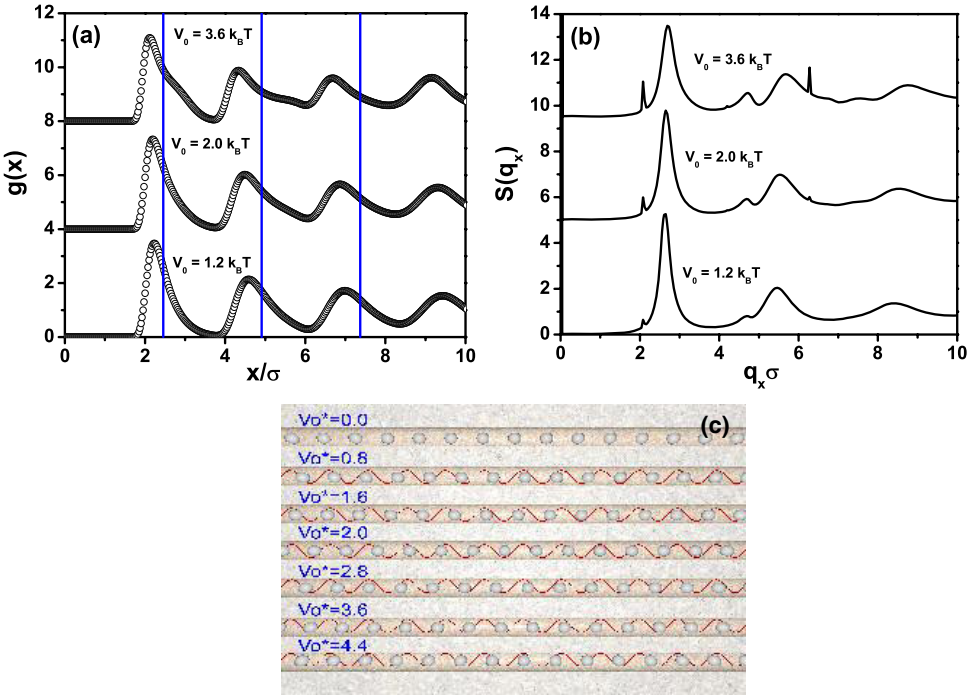

Figure 5. (a) Pair distribution functions for the case $a_L = 3\sigma$ with $\varphi \approx 0.407$ for three different substrate strengths: $V_0 = 1.2$, 2.0 and 3.6 k_BT. The perpendicular solid lines represent the position of each maximum for the case $V_0 = 0$. (b) Static structure factors. The curves are shifted for clarity. (c) From top to bottom, the substrate strengths are $V_0/k_BT = 0$, 0.8, 1.6, 2.0, 2.8, 3.6 and 4.4. The sinusoidal term of equation (9) is plotted (dashed lines) on each channel to understand the way in which the particles are positioned with respect to the substrate minima.

$p \approx 0.82$. It is evident that the $g(x)$ is not as structured, or correlated, as in the previous cases (including also the case without a substrate). In fact, the distribution functions are almost identical, although the height of the minima and maxima decrease slightly when V_0 increases. This intriguing result, in contrast to the previous cases, suggests a kind of *loss* of correlation among the particles and a possible depinning of the adsorbed particles from the sinusoidal substrate. This is confirmed by the structure factor in figure 5(b). It shows practically one peak at the position $q_x\sigma \approx 2.65$ which is related to the mean separation among particles, confirming then that the local order at short and large separations has notably decreased. On the other hand, by looking at the height of the $S(q)$ at the position $q_x\sigma = 2\pi/3$ (and integer multiples of it) one can appreciate that there are no regions of particles on the substrate minima. This is clear evidence of the depinning effect. Also, the snapshots of figure 5(c) allow to visualize that the particle positions do not change dramatically for any value of $V_0 \neq 0$. Our findings were corroborated with MC simulations (data not shown).

To illustrate the effects due to the variation in the density, we now fix the substrate periodicity to the experimental value $a_L = 5.5$ μm [19] and the substrate strength $V_0 = 3.6$ k_BT. Figure 6(a) shows the distribution function for several packing fractions, $0.288 \leqslant \varphi \leqslant 0.43$. At small densities ($\varphi < 0.3$) the particles are, on average, in each substrate minimum due to the energy per particle without substrate always being smaller than V_0 and each $g(x)$ for $\varphi < 0.3$ collapsing in the same curve (see, for example, $g(x)$ for $\varphi = 0.288$). However, at higher densities the pair interaction between particles becomes as relevant as the

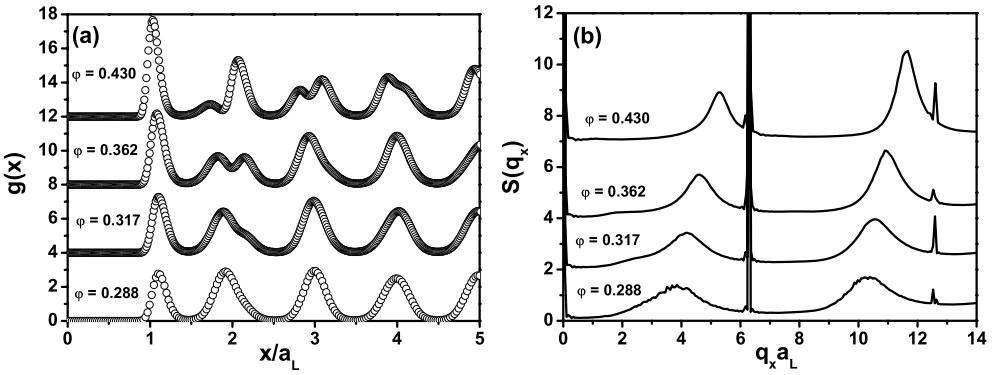

Figure 6. (a) Pair distribution functions for the case $a_L = 5.5\ \mu$m with $V_0 = 3.6\ k_BT$ for different packing fractions (from bottom to top) $\varphi = 0.288$, 0.317, 0.362 and 0.43. (b) Static structure factors. The curves are shifted for clarity.

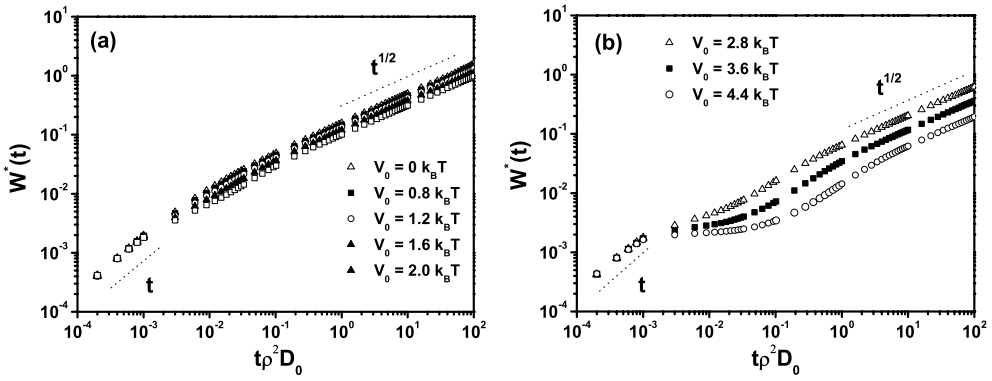

Figure 7. Reduced mean-square displacement, $W^*(t)$, for the system of figure 4 for different substrate strengths: (a) $V_0 = 0$, 0.8, 1.2, 1.6 and 2.0 k_BT; (b) $V_0 = 2.8$, 3.6 and 4.4 k_BT.

substrate–particle interaction, and therefore the competition between both interactions leads to a rich variety of incommensurate phases. The non-monotonic variation in the structure results from the fact that, for packing fractions smaller than $\varphi = 0.4$, the mean particle distance in the absence of a substrate does not scale according to the relation $d = \varphi^{-1}\sigma$ (see figure 1(a)) and then the factor p also changes in a non-monotonic fashion. Nonetheless, the structure factor in figure 6(b) also indicates that two particles can be closer or further than the distance between two consecutive substrate minima (see the peaks around the position $q_x a_L = 2\pi$).

4.3. Dynamics

The reduced mean-square displacements, $W^*(t)$, for the system described in figure 4 are shown in figure 7(a) for small substrate strengths $V_0/k_BT = 0$, 0.8, 1.2, 1.6 and 2.0, and in figure 7(b) for high substrate strengths $V_0/k_BT = 2.8$, 3.6 and 4.4. In both figures (and in all cases that we here considered), we appreciate that at sufficiently short times ($t < 10^{-3}/\rho^2 D_0$), where the individual particles do not feel direct interactions with the other colloids, normal diffusion occurs and the mean-square displacement is found to be $W(t) \propto t$. At long times, surprisingly, the diffusion law given by (1) still remains valid. For small V_0, the transition from normal

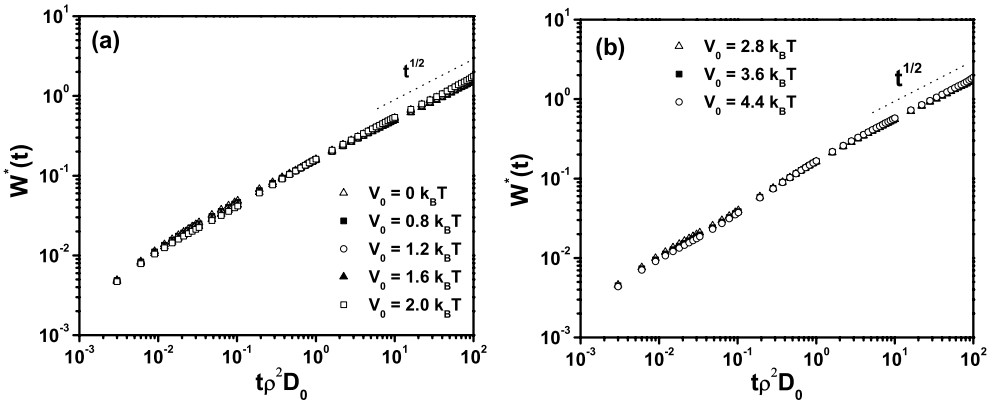

Figure 8. Reduced mean-square displacement, $W^*(t)$, for the system of figure 5 for different substrate strengths: (a) $V_0 = 0$, 0.8, 1.2, 1.6 and 2.0 k_BT; (b) $V_0 = 2.8$, 3.6 and 4.4 k_BT.

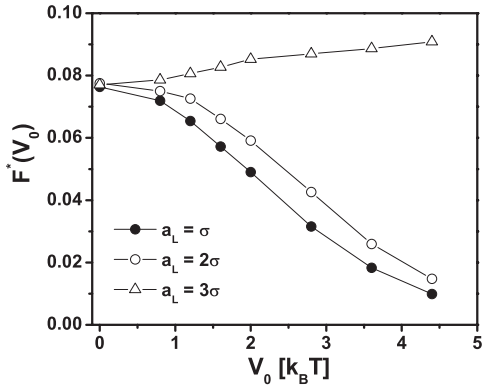

Figure 9. Reduced mobility factor, F^*, as a function of the substrate strength, V_0, for different substrate periodicities, $a_L = \sigma$, 2σ and 3σ with $\varphi = 0.407$. The line is just a guide for the eye.

diffusion to sub-diffusion occurs continuously. For high V_0, however, the diffusion of particles is severely affected by the energetic barrier created by the periodic substrate; see figure 7(b). In this case we observe that at intermediate times the particles now diffuse more slowly than at short and long times. The reduction in particle diffusion is due to the particles now having to spend a longer time jumping between several substrate minima before reaching diffusional collective motion. This causes the particles to diffuse (or oscillate) around the position of each minimum for a long period of time. At sufficiently long times, i.e. when the particles diffuse a considerable number of mean interparticle distances, the diffusion law $W(t) \propto t^{1/2}$ is recovered. However, the time needed to surmount the energetic barrier increases with the substrate strength. In fact, to reach the sub-diffusion regime at long-times, one must carefully simulate for times much longer than the typical experimental times [11, 15]. On the other hand, the mobility factor reduces when V_0 increases (see black circles in figure 9).

The results for $W(t)$ in the case $a_L = 2\sigma$ are quantitatively similar to the case discussed previously (data not shown); they show the same behaviour at all time regimes but, as is illustrated in figure 9 (open circles), the mobility factor is, in general, larger. The case $a_L = 3\sigma$ is visualized in figures 8 and 9 (open triangles). Here one can observe that, for any substrate

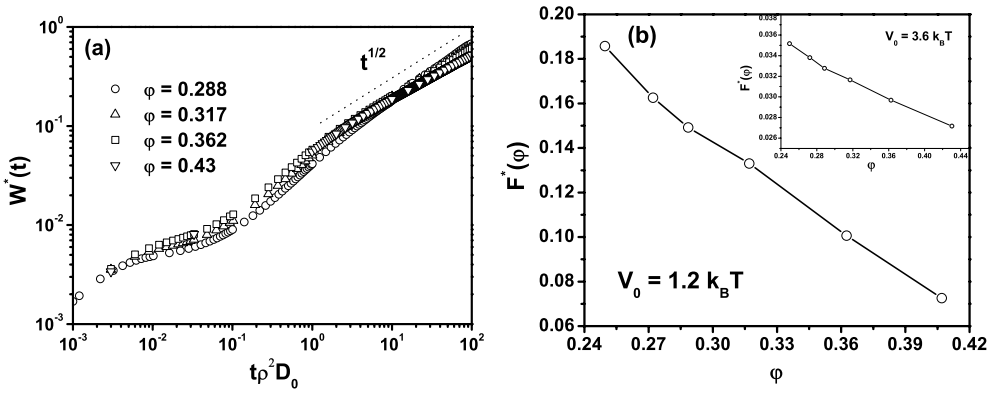

Figure 10. (a) Reduced mean-square displacement, $W^*(t)$, for the case $a_L = 5.5\ \mu$m with $V_0 = 3.6\ k_BT$ for different packing fractions: $\varphi = 0.288$, 0.317, 0.362 and 0.43. (b) Main body: reduced mobility factor F^* for $V_0 = 1.2\ k_BT$. Inset: reduced mobility factor F^* for $V_0 = 3.6\ k_BT$. The line is just a guide for the eye.

strength, $W(t)$ behaves in the same fashion as a free single-file ($V_0 = 0$), although the (small) differences can be noticed at long times. Surprisingly, the mobility factor F is enhanced and takes values larger than the case without a substrate. This effect is due to the so-called noise-assisted effect, in which the thermal fluctuations act cooperatively, leading to a higher particle mobility. This effect, already seen in the diffusion of a single Brownian particle drifting down a tilted washboard potential [23], is also responsible for the evident changes in the structure of the system that we have already discussed in figure 5. In the absence of thermal noise (FK-like models), this effect cannot take place. The enhancement of F with respect to the case without a substrate also reveals the depinning of the file from its sinusoidal substrate. Then, we have shown that the depinning can be quantified directly through a loss of correlations in the structure or an enhancement of the particle mobility factor. These results can be corroborated in experiments with light forces [19].

On the other hand, the diffusion properties illustrated in figures 7–9 seem to validate the relation (1) for the type of periodic substrate considered here. However, to have a complete understanding of the diffusion properties in this system, we must take into account density variations. Therefore, in figure 10(a) the results for $W(t)$ of the system described in figure 6 are analysed. One can immediately observe that at short and intermediate times the behaviour is basically the same as in the other cases for any filling fraction, including the asymptotic behaviour at long times, $W(t) \propto t^{1/2}$, remaining valid for packing fractions $\varphi < 0.4$. Nevertheless, for the case $\varphi = 0.43$, a strong deviation is clearly observed. This deviation can be due to the fact that at such density the particles are not able to surmount the energetic barrier imposed by the combination of both the pair interaction and the substrate. Then the time needed to reach the diffusive collective motion increases with the density, or the substrate strength. Figure 10(b) shows the mobility factor for several packing fractions with $V_0 = 1.2\ k_BT$ and $V_0 = 3.6\ k_BT$ (inset). In both cases, F decreases with density, as in the free file, but its magnitude varies according to the substrate potential.

5. Conclusions

We have investigated the structure and dynamics of charged colloidal particles in one-dimensional periodic substrates by means of Brownian dynamics simulations. In summary,

we found that:

- The competition between both the particle–particle and particle–field interactions gives rise to a rich variety of adsorbate phases or particle distributions. In particular, we observed that two colloids can be closer or further than the distance between two consecutive substrate minima.
- The non-Fickian behaviour observed experimentally and predicted theoretically by Kollmann is here corroborated and extended to the case of sinusoidal periodic substrates;
- The depinning of the particles is captured by the structure and the corresponding mobility factor. This result can be corroborated in experiments on charge-stabilized colloidal suspensions under the influence of light forces. Experiments in such a direction can also allow the determination of the file depinning threshold.

Acknowledgments

The authors thank C Bechinger and J Méndez-Alcaraz for highlighting and stimulating discussions. Financial support from the Consejo National de Ciencia y Tecnología (grant 46373/A-1) is acknowledged.

References

[1] Heinsalu E, Patriarca M, Goychuk I and Hänggi P 2007 *J. Phys.: Condens. Matter* **19** 065114
[2] Lee H Y, Lee H W and Kim D 1998 *Phys. Rev. Lett.* **81** 1130
[3] Stroock A D *et al* 2000 *Phys. Rev. Lett.* **84** 3314
[4] Kärger J and Ruthven D M 1992 *Diffusion in Zeolites and Other Microporous Solids* (New York: Wiley–Interscience)
[5] Hodgkin A L and Kenes R D 1955 *J. Physiol.* **128** 61
[6] Harris T E 1965 *J. Appl. Probab.* **2** 323
[7] Arratia A 1983 *Ann. Probab.* **11** 362
[8] Levitt D G 1973 *Phys. Rev.* A **8** 3050
[9] Kärger J 1992 *Phys. Rev.* A **45** 4173
Hahn K, Kärger J and Kukla V 1996 *Phys. Rev. Lett.* **76** 2762
[10] Kollmann M 2003 *Phys. Rev. Lett.* **90** 180602
[11] Lutz C, Kollmann M and Bechinger C 2004 *Phys. Rev. Lett.* **93** 026001
[12] Wei Q H, Bechinger C and Leiderer P 2000 *Science* **287** 625
[13] Cui B *et al* 2002 *J. Chem. Phys.* **116** 3119
[14] Lin B *et al* 2002 *Europhys. Lett.* **57** 724
[15] Lutz C, Kollmann M, Bechinger C and Leiderer P 2004 *J. Phys.: Condens. Matter* **16** S4075
[16] Taloni A and Marchesoni F 2006 *Phys. Rev. Lett.* **96** 020601
[17] Griffiths R B 1990 *Fundamental Problems in Statistical Mechanics* vol VII (Amsterdam: Elsevier)
[18] Chaikin P M and Lubensky T C 1995 *Principles of Condensed Matter Physics* (Cambridge: University Press)
[19] Bleil S, von Grünberg H H, Dobnikar J, Castañeda-Priego R and Bechinger C 2006 *Europhys. Lett.* **73** 450
[20] Hansen J P and McDonald I R 1990 *Theory of Simple Liquids* (New York: Academic)
[21] Ermak D L 1975 *J. Chem. Phys.* **62** 4189
[22] Allen M P and Tildesley D J 1987 *Computer Simulation of Liquids* (Oxford: Clarendon)
[23] Costantini C and Marchesoni F 1999 *Europhys. Lett.* **48** 491